Chapter 2

Laser Capture Microdissection as a Tool to Study Tumor Stroma

Nicholas R. Bertos and Morag Park

Abstract

Laser capture microdissection (or LCM) allows for isolation of cells from specific tissue compartments, which can then be followed by DNA, RNA, and/or protein isolation and downstream characterization. Unlike other methods for cell isolation, LCM can be directed towards cells situated in specific anatomical contexts, and is therefore of significant value when investigating the tumor microenvironment, where localization is often key to function. Here, we present a summary of ways in which LCM can be utilized, as well as protocols for the isolation of tumor and tumor-associated stromal elements from frozen breast cancer samples, with a focus on preparation of samples for RNA characterization.

Key words Laser capture microdissection, RNA profiling, Quality control, Arcturus PixCell IIe, Cell isolation

1 Introduction

Investigations of tumor stroma, specifically in the field of breast cancer, have been greatly aided by the use of laser capture microdissection (LCM). This technology has been utilized to investigate genomic [1–3], transcriptional [4–14], and protein-level [15, 16] alterations in the human breast cancer microenvironment. Work in our group has principally been carried out using breast tumors from patients and murine models, with a downstream goal of generating mRNA expression profiles and analyzing these to identify stromal influences on breast cancer development, progression, and outcome [11–14]. Importantly, the datasets generated by such experiments constitute key resources for further analyses and validation of findings from other approaches—the datasets generated from some of our studies [12, 14], for example, have been utilized to support multiple additional investigations [17–30].

Laser capture microdissection was first effectively developed in the mid-1990s as a means to rapidly isolate distinct subpopulations of cells from heterogeneous tissues under direct microscopic

Josie Ursini-Siegel and Nicole Beauchemin (eds.), *The Tumor Microenvironment: Methods and Protocols*, Methods in Molecular Biology, vol. 1458, DOI 10.1007/978-1-4939-3801-8_2, © Springer Science+Business Media New York 2016

visualization [31, 32]. The underlying principle of the initial infrared (IR) laser-based systems was the placing of a thin thermolabile transparent film over a tissue section placed on a microscope slide. Following visualization of the areas of interest, a short focused laser pulse selectively adheres the film to a small area of tissue; when the film is removed, these tissue regions remain attached and can then be isolated and subjected to downstream assays (Fig. 1). Note that the forces counteracting tissue lifting include both interactions with the slide surface and with neighboring cells; thus, for tissues with very strong intercellular adhesion, other approaches may be needed. These include the use of membrane slides where the area of interest can be cut out using a UV laser which cuts through both the sample and the membrane itself, obviating the

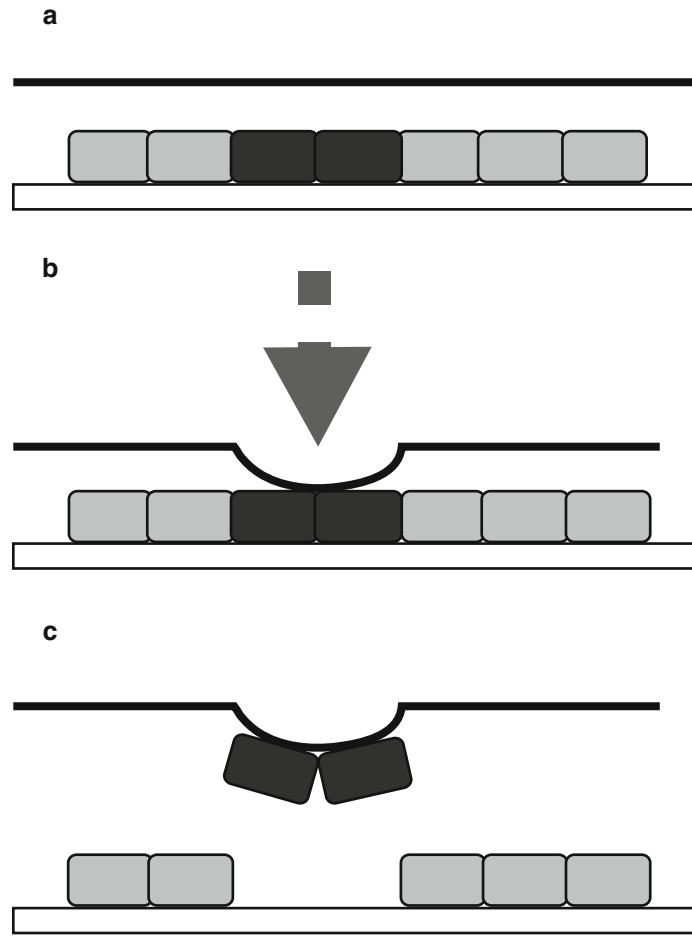

Fig. 1 Schematic image of IR-mediated LCM. (**a**) Thermolabile film (*black line*) is placed above tissue on slide (*bottom*). (**b**) Laser (*dashed line*/*arrowhead*) melts film and causes it to contact cells of interest (*dark grey*), avoiding undesired cells (*light grey*). (**c**) Film bearing cells of interest is lifted, separating these from the remaining cells

need for tissue detachment by lifting from either the slide or the neighboring tissue. A somewhat different technology is used in the laser catapult system (e.g., Zeiss PALM MicroBeam), where a UV laser is used to both cut around the region of interest, and to subsequently "catapult" the excised tissue into a collection cap.

Among existing means for isolating specific cell subpopulations from heterogeneous samples, LCM stands out due to the ability to select cells based on their anatomical context. Fluorescence-activated cell sorting and antibody-bead conjugate-based systems are agnostic with respect to cell localization within a tissue context, while manual microdissection is limited to relatively large areas of interest. Identification of cells for targeted isolation by LCM can be conducted either by standard staining and visual identification or by immunohistochemistry- or immunofluorescence-guided selection.

Since its initial development, various permutations of LCM have been developed, including the use of an ultraviolet (UV) cutting laser either alone or in conjunction with the IR laser. UV lasers are used to ablate unwanted tissue, cut around regions of thick or adherent tissues so that these can be detached using IR laser-mediated adhesion (or isolated separately in the case of sections mounted on membrane slides), and/or to catapult isolated regions into a retrieval container. Semiautomated methods for identification of regions to be isolated are also under development [33].

Candidate materials for LCM include frozen tissue as well as formalin-fixed paraffin-embedded (FFPE) samples—note that staining protocols must be modified for FFPE samples, due to the requirement for deparaffinization. Cytology smears and live cells have also been targeted for this approach. Depending on cell and tissue type and isolation desired, yields can vary widely; pilot experiments should be conducted to determine how much LCM is required to obtain desired target quantities when working with a new experimental system.

Especially for RNA isolation and downstream assays, the importance of maintaining a clean working environment cannot be overstated. The use of dedicated space and equipment, including cryostats for sample preparation, reduces the chances of sample degradation (e.g., by RNase used on adjacent benches) and cross-contamination. In addition, LCM efficacy can be influenced by environmental conditions. Humidity levels above 50% lead to increased adhesion between the tissue section and the slide, which can make it impossible to isolate the selected regions. If room humidity is too high, then the use of a portable dehumidifier may be necessary,

In our experience, the time elapsed between tissue isolation from the organism and initial freezing is key to sample quality and assay success. For human clinical breast tumor samples, we have found that times in excess of 30 min are generally associated with failure to isolate RNA of acceptable quality following LCM;

however, the precise timing is likely to vary between tissues and LCM protocols used, and should be determined experimentally for each experimental condition.

Our standard operating procedure is to immediately place tissue samples obtained in a cryovial (Nalgene) containing ca. 1 mL of Tissue-Tek O.C.T. Compound ("O.C.T.," Sakura Finetek, USA), cover them with additional O.C.T., and then rapidly freeze the vial in liquid nitrogen. Although samples can be frozen directly and later mounted in O.C.T. prior to sectioning, this entails additional manipulation and risks loss of sample morphology. Other approaches that better preserve tissue morphology involve fixation in 4% paraformaldehyde or in ethanol on ice prior to equilibration in O.C.T. and less rapid freezing. However, some RNA degradation may occur with the latter approaches—comparative pilot studies for the tissue and target of interest should be conducted prior to beginning work to achieve the optimal balance of morphology vs. sample preservation required. Samples can then be stored at –80 °C or in liquid nitrogen until use; in our experience, storage times of up to 15 years in liquid nitrogen do not affect RNA integrity.

O.C.T.-embedded samples are then sectioned at 10 μm thickness using a cryostat, taking care to place tissue sections in the central third of the slide. We have found that for breast tumor tissue, this represents an acceptable balance between maximizing LCM yields and ensuring that the area visualized corresponds to what is isolated, since in thicker sections cells lying beneath the visible layer may be co-isolated. For tissue with higher degrees of local heterogeneity, thinner sections may be required; however, these would require more LCM processing to isolate the same amount of tissue. It is important to ensure that samples and sections are kept as cold as possible during this procedure; this entails pre-cooling slide boxes before use, and transferring cut sections into these within the cryostat chamber, as well as always transporting sections in insulated containers with dry ice. To minimize the potential for cross-contamination, the cryostat chamber should be vacuumed between samples, surfaces should be cleaned with acetone, and a fresh blade should be used for each sample. Sections on slides are stored at –80 °C until use. The time for which slides can be stored depends on tissue type and intended use—for human breast tumor samples, 2–3 months is generally the limit for subsequent RNA isolation.

Two key elements in successful LCM-mediated isolation of tissue for downstream analysis are the quality of the input material, and optimization of the protocol to minimize loss of integrity during the procedure. Since LCM is carried out at room temperature, further sample degradation can occur during the procedure; thus, initial sample quality must be carefully assessed, and samples must be followed throughout the procedure.

Our workflow integrates multiple quality control steps designed to avoid additional processing of poor-quality samples. In addition, stepwise assays of sample quality allow for identification of steps leading to sample degradation which may require modification.

First, tissue from four to five slides bearing sectioned samples is manually isolated and subjected to RNA isolation as per the protocol below, followed by quality assessment using the RNA Pico kit on the Agilent Bioanalyzer platform. Next, tissue-bearing slides that have been stained as per the protocol to be used in the study in question are similarly processed to identify samples which deteriorate to an unusable point during the staining step. Samples for which RNA is not of acceptable quality after sectioning or staining are removed from the workflow. As a final step prior to LCM performance, stained sections are exposed to room temperature for times corresponding to expected LCM duration, and similarly processed—this identifies samples for which LCM processing time may require adjustment.

2 Materials

2.1 Total RNA Extraction for Quality Control

1. TRIzol (ThermoFisher).
2. Glycogen (GenHunter).
3. Chloroform.
4. Isopropanol.
5. Ice-cold 75 % ethanol.
6. RNase-free water.
7. 1.5 mL tubes.
8. Pipettor and tips.
9. Vortex mixer.
10. Centrifuge capable of 12,000 × *g* and refrigerated at 4 °C.

2.2 H&E Staining for LCM

Note: Sections should not be allowed to dry out during staining procedures.

1. Harris hematoxylin (Surgipath).
2. Eosin (Surgipath).
3. 70 %, 95 %, and 100 % ethanol.
4. Xylene.
5. RNase-free water.
6. Bluing solution: 0.3 % Ammonium hydroxide.
7. 0.22 μm Filter (Steritop system, Millipore).
8. RNase-free glass surface.
9. RNase-free staining jars.

2.3 HistoGene Staining

Note: Sections should not be allowed to dry out during the procedure.

1. HistoGene staining kit (Life Technologies catalog # KIT0401; this contains all required reagents and consumables).
2. RNase-free glass surface.
3. RNase-free tweezers and forceps to manipulate slides.

2.4 Laser Capture Microdissection

Note: The procedure below is written for the Arcturus PixCell IIe system, which utilizes an IR laser only. Other systems exist which incorporate IR and/or UV lasers; for these, carefully following the manufacturer's directions is recommended.

1. Arcturus PixCell IIe LCM system.
2. CapSure caps.
3. Tissue on slides.
4. 100% Ethanol and lint-free wipes to clean work area.
5. PrepStrips (Arcturus).
6. CapSure cleanup pads (*see* **Note 1**).

3 Methods

3.1 Total RNA Extraction for Quality Control

1. Prepare a 1.5 mL tube with 1 mL of TRIzol (ThermoFisher).
2. Pipette ca. 200 μL of TRIzol onto each section.
3. Pipette TRIzol up and down over the section several times.
4. Transfer material to TRIzol-containing tube.
5. Vortex briefly to homogenize tissue. Samples can now be stored at −80 °C prior to extraction. Prior to proceeding to next step, thaw frozen samples and incubate at room temperature for 5 min.
6. Add 200 μL of chloroform and shake vigorously by hand for 15 s.
7. Incubate at room temperature for 3 min.
8. Centrifuge at 12,000 × *g* for 15 min at room temperature.
9. Transfer upper aqueous phase (400–450 μL) to a new 1.5 mL tube.
10. Precipitate RNA by adding 500 μL of isopropanol and 2 μL of glycogen.
11. Mix by manually inverting ten times, and then incubate for 10 min at room temperature.
12. Centrifuge at 12,000 × *g* for 10 min at 4 °C.
13. Carefully remove and discard supernatant.
14. Add 1 mL ice-cold 75% ethanol (wash step) and shake tube.

15. Centrifuge at 7500 × *g* for 5 min at 4 °C.
16. Carefully remove ethanol and air-dry pellet for 10–15 min at room temperature.
17. Resuspend pellet in 15 μL RNase-free water and incubate at 55 °C for 10 min to dissolve pellet.
18. Proceed to RNA assay, e.g., using the Bioanalyzer platform.

3.2 H&E Staining for LCM

We currently utilize either the Arcturus HistoGene LCM Frozen Section Staining Kit (Applied Biosystems) or an in-house hematoxylin and eosin (H&E)-based procedure for sample staining. Both procedures are listed below; the HistoGene kit has the advantage of not requiring manual preparation of solutions, albeit at higher cost. Also, sections stained using H&E are more easily interpretable for outside experts called in to analyze samples, i.e., pathologists, while the brown staining obtained with the HistoGene kit requires some familiarization.

1. Filter Harris hematoxylin prior to use using a 0.22 μm filter to remove any precipitate.
2. Thaw slides at room temperature on an RNase-free glass surface (to ensure even thawing) for a maximum of 30 s.
3. Fix slides with 70% ethanol for 30 s.
4. Rinse slides with two rapid dips in RNase-free water.
5. Stain slides with hematoxylin for 30 s.
6. Rinse slides with one rapid dip in RNase-free water.
7. Blue in 0.3% ammonium hydroxide solution for 30 s.
8. Dehydrate by placing slides in 70% ethanol (2 × 30 s), followed by 95% ethanol (2 × 30 s).
9. Stain slides with eosin (Surgipath) for 20 s.
10. Dehydrate slides using through 30-s steps in 95% ethanol (2 × 30 s), 100% ethanol (2 × 30 s), and xylene (60 and 90 s).
11. Air-dry slides for 10 min in a fume hood.
12. Use slides immediately for LCM—if multiple slides have been stained and will be used in the same LCM session, the extra sections can be stored in a cold desiccator until use.

3.3 HistoGene Staining

Note: Adapted from the manufacturer's instructions.

1. Thaw slides at room temperature on an RNase-free glass surface for a maximum of 30 s.
2. Fix slides in 75% ethanol for 30 s.
3. Rinse in RNase-free water for 30 s.
4. Apply 100 μL of HistoGene staining solution to each section and place on a glass surface for 20 s.

5. Rinse in RNase-free water for 30 s.
6. Dehydrate slides by dipping in 75 % ethanol for 30 s, 95 % ethanol for 30 s, and 100 % ethanol for 30 s.
7. Clear sections by dipping in xylene for 5 min.
8. Air-dry slides in a fume hood for 5 min.
9. Use slides immediately for LCM—if multiple slides have been stained and will be used in the same LCM session, extra sections can be stored in a cold desiccator until use.

3.4 Laser Capture Microdissection

Note: Adapted from the manufacturer's instructions.

1. Turn on power to the instrument, controller, and computer.
2. If using fluorescence, turn on power to Olympus mercury lamp and close the fluorescence shutter until you are ready to view fluorescent samples (*see* **Notes 2**–**5**).
3. Dust off working surfaces with compressed air and spray with 100 % ethanol. Wipe off excess ethanol with lint-free wipes (e.g., Kimwipes).
4. Load CapSure caps (HS or Macro) in the CapSure cassette module (*see* **Note 6**).
5. Remove possible debris from the section surface using Arcturus PrepStrips.
6. Center the joystick in the vertical position and place the sample slide onto the stage.
7. Identify a region with cells of interest. Place it on the center of the field of view (*see* **Note 7**). Activate the vacuum button on the front of the laser controller (*see* **Note 8**). Make sure that a cap is at the load line position.
8. Without lifting the Cap Placement Arm, rotate it to the cap pickup position. The arm will automatically line up with the cap.
9. Lift the arm with the cap and turn it slowly clockwise until it stops.
10. Lower arm to place the cap on the tissue section, on the region of interest.
11. Adjust the fine focus on microscope and adjust light intensity. Examine the sample, moving around using the joystick.
12. Initiate archiving software. Enter the file name, study name, and slide number, adding notes if necessary.
13. Take "map" (low power, whole section) and "before" (higher power, area to be microdissected) images if desired (Fig. 2) (*see* **Note 9**). Set laser parameters, and then activate laser by turning key clockwise. Once laser interlock check is complete, turn on laser using the "laser enable" button (*see* **Note 10**).

14. To focus the laser, go to the 20× objective, adjust the microscope focus, and decrease the light sufficiently to see the laser spot on the monitor. Move to an open space close to tissue and fire test shots, adjusting laser focus knob until you observe an optimal laser spot (*see* **Note 11**).
15. Reset the pulse number to zero before starting LCM on sample.
16. Position the laser targeting spot over the cells of interest and fire the laser. Move the stage with the joystick and continue firing laser to collect all required material.
17. Raise the Cap Placement Arm with the cap and move it gently to the rest position.
18. Observe remaining tissue on the slide and take "after" images of dissected regions.
19. To observe captured cells, turn off vacuum and remove the slide from stage. Change the objective to low magnification. Gently turn the capping arm clockwise, placing the cap in the center of the field of vision. Examine the cap at low and high magnification, collecting "cap" images, if needed (Fig. 2) (*see* **Note 12**). Using capping tool, transfer the cap with captured cells onto a 1.5 mL tube with appropriate extraction buffer.
20. When finished with LCM procedures, turn off vacuum and laser (turn key counterclockwise), close archiving software, and turn off controller.
21. Remove consumables and cover microscope (*see* **Note 13**).

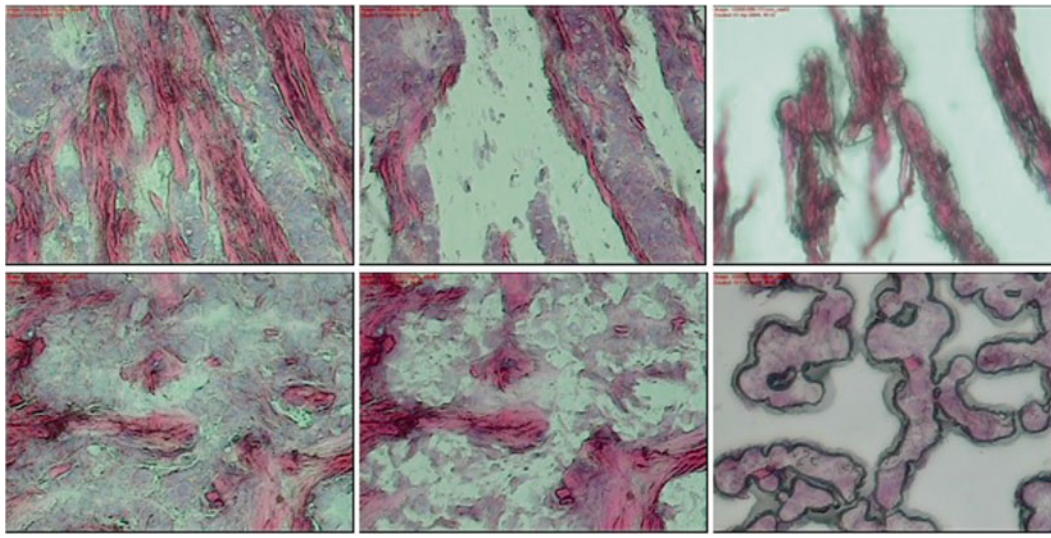

Fig. 2 "Before" (*left*), "after" (*centre*), and "cap" (*right*) images of laser capture microdissection for tumor-associated stroma (*top row*) and tumor epithelium (*bottom row*)

4 Notes

1. These are no longer commercially available; adhesive notes can be used as a substitute.
2. Note that it takes time for the mercury lamp to become stable; turn it on 20–30 min before starting to perform LCM.
3. The fluorescence cube turret is located under the stage. It has four positions for blue, green, and orange filter cubes plus a bright-field position (white light, no color filter cube). Select the position with the appropriate color filter by rotating the cube turret.
4. The cube turret has a built-in shutter. The shutter should always remain closed unless viewing fluorescent samples. Leaving the shutter opened for extended periods will photobleach fluorescent dyes.
5. The "normal" position on the control box is used for routine procedures (no fluorescence or strong fluorescence). For samples with weak fluorescence, it is possible to enhance the signal intensity by increasing the integration time from "normal" to the minimum setting which is needed to observe a good signal from the sample. The white light setting should remain very low.
6. HS caps include a standoff rail that keeps the thermolabile film above the tissue surface, while Macro caps do not. Use of HS caps reduces potential contamination of the film at the expense of reducing total possible yield.
7. Ideal work area should have both open space for laser test firing and cells of interest for dissection.
8. The vacuum acts to hold the slide in place on the stage.
9. Images can be saved in .jpg or .tif formats; saving as .tif files uses more disk space (ca. 1 Mb/image vs. ca. 300 kb for .jpg images).
10. Although each procedure will require individual optimization, a useful set of initial settings for mammary tissue is as follows: spot size 15 μm, target voltage 0.2 V, current 4.4 mA, and power 25 mW.
11. Proper film melting is occurring if you observe a black ring around the spot. If this ring is not observed, adjust laser focus and power until it is observed (Fig. 3).
12. If contamination with non-dissected material is observed on cap, clean it very gently with CapSure pad.
13. In many cases, individuals who have been performing LCM for the first time have reported vertigo and/or nausea following protracted LCM sessions. This is likely an effect of intently

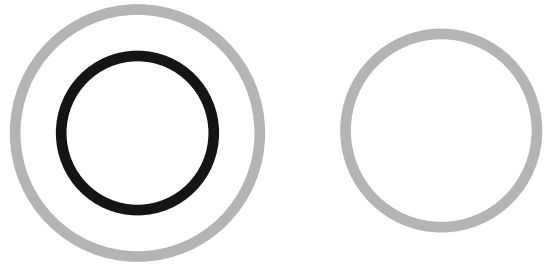

Fig. 3 Schematic images of correct (*left*) and incorrect (*right*) laser pulses. In *the left-hand image*, the thermolabile film is in contact with the tissue below, while in *the right-hand image*, contact has not been achieved

watching the computer screen as it rapidly displays movement across different regions of the specimen. Increased experience with the procedure reduces but does not completely abolish this effect. Taking short breaks every 30 min may be useful.

Acknowledgements

This work was supported by funding from the Database and Tissue Bank Axis of the "Réseau de Recherche sur le Cancer" of the "Fonds de Recherche du Québec-Santé" and the Québec Breast Cancer Foundation to M.P.

References

1. Wernert N, Locherbach C, Wellmann A, Behrens P, Hugel A (2000) Presence of genetic alterations in microdissected stroma of human colon and breast cancers. J Mol Med 78(7):B30
2. Kurose K, Hoshaw-Woodard S, Adeyinka A, Lemeshow S, Watson PH, Eng C (2001) Genetic model of multi-step breast carcinogenesis involving the epithelium and stroma: clues to tumour-microenvironment interactions. Hum Mol Genet 10(18):1907–1913
3. Ellsworth DL, Ellsworth RE, Love B, Deyarmin B, Lubert SM, Mittal V, Shriver CD (2004) Genomic patterns of allelic imbalance in disease free tissue adjacent to primary breast carcinomas. Breast Cancer Res Treat 88(2):131–139. doi:10.1007/s10549-004-1424-7
4. Boersma BJ, Reimers M, Yi M, Ludwig JA, Luke BT, Stephens RM, Yfantis HG, Lee DH, Weinstein JN, Ambs S (2008) A stromal gene signature associated with inflammatory breast cancer. Int J Cancer 122(6):1324–1332. doi:10.1002/ijc.23237
5. Ma XJ, Dahiya S, Richardson E, Erlander M, Sgroi DC (2009) Gene expression profiling of the tumor microenvironment during breast cancer progression. Breast Cancer Res 11(1):R7. doi:10.1186/bcr2222
6. Martin DN, Boersma BJ, Yi M, Reimers M, Howe TM, Yfantis HG, Tsai YC, Williams EH, Lee DH, Stephens RM, Weissman AM, Ambs S (2009) Differences in the tumor microenvironment between African-American and European-American breast cancer patients. PLoS One 4(2):e4531. doi:10.1371/journal.pone.0004531
7. Witkiewicz AK, Kline J, Queenan M, Brody JR, Tsirigos A, Bilal E, Pavlides S, Ertel A, Sotgia F, Lisanti MP (2011) Molecular profiling of a lethal tumor microenvironment, as defined by stromal caveolin-1 status in breast cancers. Cell Cycle 10(11):1794–1809
8. Planche A, Bacac M, Provero P, Fusco C, Delorenzi M, Stehle JC, Stamenkovic I (2011) Identification of prognostic molecular features

in the reactive stroma of human breast and prostate cancer. PLoS One 6(5):e18640. doi:10.1371/journal.pone.0018640

9. Harvell DM, Kim J, O'Brien J, Tan AC, Borges VF, Schedin P, Jacobsen BM, Horwitz KB (2013) Genomic signatures of pregnancy-associated breast cancer epithelia and stroma and their regulation by estrogens and progesterone. Horm Cancer 4(3):140–153. doi:10.1007/s12672-013-0136-z
10. Winslow S, Leandersson K, Edsjo A, Larsson C (2015) Prognostic stromal gene signatures in breast cancer. Breast Cancer Res 17:23. doi:10.1186/s13058-015-0530-2
11. Ponzo MG, Lesurf R, Petkiewicz S, O'Malley FP, Pinnaduwage D, Andrulis IL, Bull SB, Chughtai N, Zuo D, Souleimanova M, Germain D, Omeroglu A, Cardiff RD, Hallett M, Park M (2009) Met induces mammary tumors with diverse histologies and is associated with poor outcome and human basal breast cancer. Proc Natl Acad Sci U S A 106(31):12903–12908. doi:10.1073/pnas.0810402106
12. Finak G, Bertos N, Pepin F, Sadekova S, Souleimanova M, Zhao H, Chen H, Omeroglu G, Meterissian S, Omeroglu A, Hallett M, Park M (2008) Stromal gene expression predicts clinical outcome in breast cancer. Nat Med 14(5):518–527. doi:10.1038/nm1764
13. Pepin F, Bertos N, Laferriere J, Sadekova S, Souleimanova M, Zhao H, Finak G, Meterissian S, Hallett MT, Park M (2012) Gene expression profiling of microdissected breast cancer microvasculature identifies distinct tumor vascular subtypes. Breast Cancer Res 14(4):R120. doi:10.1186/bcr3246
14. Finak G, Sadekova S, Pepin F, Hallett M, Meterissian S, Halwani F, Khetani K, Souleimanova M, Zabolotny B, Omeroglu A, Park M (2006) Gene expression signatures of morphologically normal breast tissue identify basal-like tumors. Breast Cancer Res 8(5):R58. doi:10.1186/bcr1608
15. Hildenbrand R, Schaaf A, Dorn-Beineke A, Allgayer H, Sutterlin M, Marx A, Stroebel P (2009) Tumor stroma is the predominant uPA-, uPAR-, PAI-1-expressing tissue in human breast cancer: prognostic impact. Histol Histopathol 24(7):869–877
16. Reddy LA, Mikesh L, Moskulak C, Harvey J, Sherman N, Zigrino P, Mauch C, Fox JW (2014) Host response to human breast Invasive Ductal Carcinoma (IDC) as observed by changes in the stromal proteome. J Proteome Res 13(11):4739–4751. doi:10.1021/pr500620x
17. Liu S, Umezu-Goto M, Murph M, Lu Y, Liu W, Zhang F, Yu S, Stephens LC, Cui X, Murrow G, Coombes K, Muller W, Hung MC, Perou CM, Lee AV, Fang X, Mills GB (2009) Expression of autotaxin and lysophosphatidic acid receptors increases mammary tumorigenesis, invasion, and metastases. Cancer Cell 15(6):539–550. doi:10.1016/j.ccr.2009.03.027
18. Bronisz A, Godlewski J, Wallace JA, Merchant AS, Nowicki MO, Mathsyaraja H, Srinivasan R, Trimboli AJ, Martin CK, Li F, Yu L, Fernandez SA, Pecot T, Rosol TJ, Cory S, Hallett M, Park M, Piper MG, Marsh CB, Yee LD, Jimenez RE, Nuovo G, Lawler SE, Chiocca EA, Leone G, Ostrowski MC (2012) Reprogramming of the tumour microenvironment by stromal PTEN-regulated miR-320. Nat Cell Biol 14(2):159–167. doi:10.1038/ncb2396
19. Pickup MW, Laklai H, Acerbi I, Owens P, Gorska AE, Chytil A, Aakre M, Weaver VM, Moses HL (2013) Stromally derived lysyl oxidase promotes metastasis of transforming growth factor-beta-deficient mouse mammary carcinomas. Cancer Res 73(17):5336–5346. doi:10.1158/0008-5472.CAN-13-0012
20. Valencia T, Kim JY, Abu-Baker S, Moscat-Pardos J, Ahn CS, Reina-Campos M, Duran A, Castilla EA, Metallo CM, Diaz-Meco MT, Moscat J (2014) Metabolic reprogramming of stromal fibroblasts through p62-mTORC1 signaling promotes inflammation and tumorigenesis. Cancer Cell 26(1):121–135. doi:10.1016/j.ccr.2014.05.004
21. Masiero M, Simoes FC, Han HD, Snell C, Peterkin T, Bridges E, Mangala LS, Wu SY, Pradeep S, Li D, Han C, Dalton H, Lopez-Berestein G, Tuynman JB, Mortensen N, Li JL, Patient R, Sood AK, Banham AH, Harris AL, Buffa FM (2013) A core human primary tumor angiogenesis signature identifies the endothelial orphan receptor ELTD1 as a key regulator of angiogenesis. Cancer Cell 24(2):229–241. doi:10.1016/j.ccr.2013.06.004
22. Shimoda M, Principe S, Jackson HW, Luga V, Fang H, Molyneux SD, Shao YW, Aiken A, Waterhouse PD, Karamboulas C, Hess FM, Ohtsuka T, Okada Y, Ailles L, Ludwig A, Wrana JL, Kislinger T, Khokha R (2014) Loss of the Timp gene family is sufficient for the acquisition of the CAF-like cell state. Nat Cell Biol 16(9):889–901. doi:10.1038/ncb3021
23. Scherz-Shouval R, Santagata S, Mendillo ML, Sholl LM, Ben-Aharon I, Beck AH, Dias-Santagata D, Koeva M, Stemmer SM, Whitesell L, Lindquist S (2014) The reprogramming of tumor stroma by HSF1 is a potent enabler of malignancy. Cell 158(3):564–578. doi:10.1016/j.cell.2014.05.045
24. Ghosh S, Ashcraft K, Jahid MJ, April C, Ghajar CM, Ruan J, Wang H, Foster M, Hughes DC,

Ramirez AG, Huang T, Fan JB, Hu Y, Li R (2013) Regulation of adipose oestrogen output by mechanical stress. Nat Commun 4:1821. doi:10.1038/ncomms2794

25. Wolford CC, McConoughey SJ, Jalgaonkar SP, Leon M, Merchant AS, Dominick JL, Yin X, Chang Y, Zmuda EJ, O'Toole SA, Millar EK, Roller SL, Shapiro CL, Ostrowski MC, Sutherland RL, Hai T (2013) Transcription factor ATF3 links host adaptive response to breast cancer metastasis. J Clin Invest 123(7):2893–2906. doi:10.1172/JCI64410
26. Liu X, Nugoli M, Laferriere J, Saleh SM, Rodrigue-Gervais IG, Saleh M, Park M, Hallett MT, Muller WJ, Giguere V (2011) Stromal retinoic acid receptor beta promotes mammary gland tumorigenesis. Proc Natl Acad Sci U S A 108(2):774–779. doi:10.1073/pnas.1011845108
27. Becker MA, Hou X, Harrington SC, Weroha SJ, Gonzalez SE, Jacob KA, Carboni JM, Gottardis MM, Haluska P (2012) IGFBP ratio confers resistance to IGF targeting and correlates with increased invasion and poor outcome in breast tumors. Clin Cancer Res 18(6):1808–1817. doi:10.1158/1078-0432.CCR-11-1806
28. Luga V, Zhang L, Viloria-Petit AM, Ogunjimi AA, Inanlou MR, Chiu E, Buchanan M, Hosein AN, Basik M, Wrana JL (2012) Exosomes mediate stromal mobilization of autocrine Wnt-PCP signaling in breast cancer cell migration. Cell 151(7):1542–1556. doi:10.1016/j.cell.2012.11.024
29. Wallace JA, Li F, Balakrishnan S, Cantemir-Stone CZ, Pecot T, Martin C, Kladney RD, Sharma SM, Trimboli AJ, Fernandez SA, Yu L, Rosol TJ, Stromberg PC, Lesurf R, Hallett M, Park M, Leone G, Ostrowski MC (2013) Ets2 in tumor fibroblasts promotes angiogenesis in breast cancer. PLoS One 8(8):e71533. doi:10.1371/journal.pone.0071533
30. Garbe JC, Pepin F, Pelissier FA, Sputova K, Fridriksdottir AJ, Guo DE, Villadsen R, Park M, Petersen OW, Borowsky AD, Stampfer MR, Labarge MA (2012) Accumulation of multipotent progenitors with a basal differentiation bias during aging of human mammary epithelia. Cancer Res 72(14):3687–3701. doi:10.1158/0008-5472.CAN-12-0157
31. Emmert-Buck MR, Bonner RF, Smith PD, Chuaqui RF, Zhuang Z, Goldstein SR, Weiss RA, Liotta LA (1996) Laser capture microdissection. Science 274(5289):998–1001
32. Bonner RF, Emmert-Buck M, Cole K, Pohida T, Chuaqui R, Goldstein S, Liotta LA (1997) Laser capture microdissection: molecular analysis of tissue. Science 278(5342):1481–1483
33. Roy Chowdhuri S, Hanson J, Cheng J, Rodriguez-Canales J, Fetsch P, Balis U, Filie AC, Giaccone G, Emmert-Buck MR, Hipp JD (2012) Semiautomated laser capture microdissection of lung adenocarcinoma cytology samples. Acta Cytol 56(6):622–631. doi:10.1159/000342984